

Damping of Confined Modes in a Ferromagnetic Thin Insulating Film: Angular Momentum Transfer Across a Nanoscale Field-defined Interface

Rohan Adur, Chunhui Du, Hailong Wang, Sergey A. Manuilov, Vidya P. Bhallamudi, Chi Zhang, Denis V. Pelekhov, Fengyuan Yang,* and P. Chris Hammel†
 Department of Physics, The Ohio State University, Columbus OH 43210, USA
 (Dated: December 6, 2024)

We observe a dependence of the damping of a confined mode of precessing ferromagnetic magnetization on the size of the mode. The micrometer-scale mode is created within an extended, unpatterned YIG film by means of the intense local dipolar field of a micromagnetic tip. We find that damping of the confined mode scales like the surface-to-volume ratio of the mode, indicating an interfacial damping effect (similar to spin pumping) due to the transfer of angular momentum from the confined mode to the spin sink of ferromagnetic material in the surrounding film. Though unexpected for insulating systems, the measured spin mixing conductance $g_{\uparrow\downarrow} = 5.3 \times 10^{19} \text{m}^{-2}$ demonstrates efficient angular momentum transfer.

Spin pumping driven by ferromagnetic resonance (FMR) is a powerful and well-established technique for generating pure spin currents in magnetic multilayers [1–3]. Understanding the mechanism that couples precessing magnetization to spin transport is an important step in utilizing this phenomenon. In addition, probing the effect of spin pumping on the damping of individual nanostructures is vital for the development of practical spintronic devices, such as spin-torque oscillators [4, 5]. Conventional FMR studies at these sub-micron length-scales becomes difficult due to the confounding effects arising from interfaces in multilayer materials and from sensitivity limitations in detecting lateral transport in single component systems at these length scales. Recent studies have shown that individual nanoscale elements exhibit size-dependent effects, such as nonlocal damping from edge modes [6] and wavevector-dependent damping in perpendicular standing spin wave modes [7]. These experiments have revealed the effect of intralayer spin pumping due to the transfer of angular momentum from regions of precession to neighboring static regions by a spin current within the same material.

A primary challenge in this endeavor is distinguishing intralayer spin pumping from other mechanisms that cause variations in linewidth from sample to sample, such as surface and edge damage [8, 9]. In this paper we measure size-dependent angular momentum transport in a single sample and in the absence of growth-defined interfaces or lithography-induced edge damage. This is achieved by confining the magnetization precession to a mode within an area defined by the controllable dipolar field from a nearby micron-sized magnetic particle [10]. This enables a unique investigation of changes in relaxation due to angular momentum transfer across the field-defined interface between precessing magnetization within a mode to the spin sink of the surrounding quiescent material.

We investigate the size dependence of interfacial damping using the technique of localized mode ferromagnetic resonance force microscopy (FMRFM) [10]. By adjusting the magnitude of the dipolar field from the probe we can

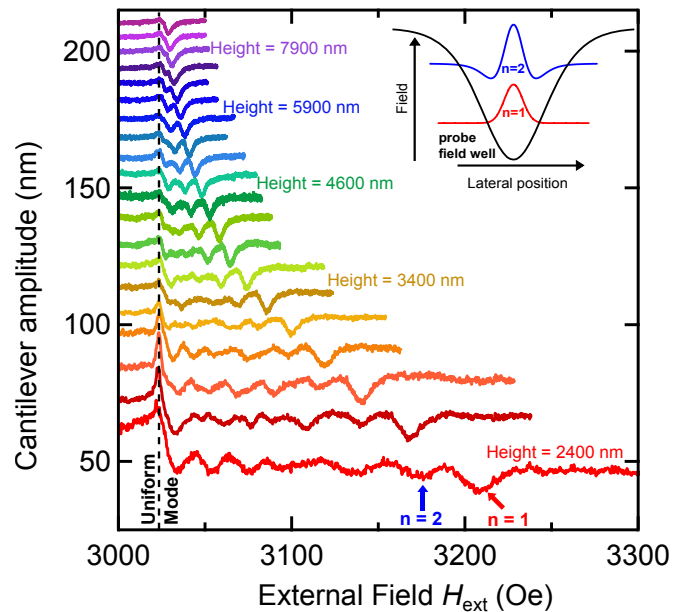


FIG. 1. Localized mode FMRFM spectra for thin film YIG at several probe-sample separations. The dashed line indicates the position of the uniform mode peak that does not shift with probe-sample separation. As probe-sample separation is reduced the localized modes shift to higher field relative to the uniform mode peak. Inset: transverse magnetization of the first two spin wave modes confined by the magnetic field well of the probe magnet. The energy of the confined modes is dictated by the depth of the field well.

control the confinement radius. Localized modes have previously been observed in permalloy when the probe field is out-of-plane [10], in-plane [11] and at intermediate angles [12]. The azimuthal symmetry of the out-of-plane geometry permits simple numerical analysis based on cylindrically symmetric Bessel function modes with a well-defined localization radius [10], similar to those seen in perpendicularly magnetized dots [13]. In addition, this geometry eliminates the effect of eigenmode splitting, which can cause additional broadening [14].

We demonstrate the control of confinement radius by

the observation of discrete modes in an FMRFM experiment in the out-of-plane geometry in an unpatterned epitaxial yttrium iron garnet (YIG) film of thickness 25 nm grown by off-axis sputtering [15] on a (111)-oriented $\text{Gd}_3\text{Ga}_5\text{O}_{12}$ substrate. The probe field is provided by a high coercivity Sm_1Co_5 particle that is milled to 1.75 μm after being mounted on an uncoated diamond atomic force microscope cantilever. The magnetic moment and coercivity of the particle are measured by cantilever magnetometry to be 3.9×10^{-9} emu and 10 kOe respectively. When the applied field is anti-parallel to the tip moment, the tip creates a confining field well in the sample that localizes discrete magnetization precession modes immediately beneath it [10, 16], analogous to the discrete modes in a quantum well [17]. The microwave frequency magnetic field that excites the precession is provided by placing the sample near a short in a microstrip transmission line. A force-detected ferromagnetic resonance spectrum is obtained by modulating the amplitude of the microwaves at the cantilever frequency (≈ 18 kHz) and measuring the change in cantilever amplitude as a function of swept external magnetic field. Measurements were made over a range of microwave frequencies: 2-6.5 GHz.

Figure 1 shows the evolution of the FMRFM spectra as a function of tip-sample separation obtained at a particular microwave frequency of 4 GHz. At large probe-sample separation we observe a peak at the expected resonance field for the uniform mode in the out-of-plane geometry. As expected [10], several discrete peaks emerge and shift toward higher applied field as the probe-sample separation decreases, thus increasing the (negative) probe field at the sample, while the uniform mode stays at constant resonance field. The resonance frequency ω of a confined mode for wavevectors $kt \ll 1$ is given by [10]

$$\frac{\omega}{\gamma} = H_{\text{ext}} - 4\pi M_s + \langle H_p \rangle + \pi M_s kt + 4\pi M_s a_{ex} k^2 \quad (1)$$

where $\gamma = 2\pi \times 2.8$ MHz/Oe is the gyromagnetic ratio, H_{ext} is the external applied magnetic field, $4\pi M_s = 1608$ Oe is the saturation magnetization, $\langle H_p \rangle$ is the negative dipole field from the probe magnet averaged over the mode, $a_{ex} = 3.6 \times 10^{-12}$ cm² is the exchange constant of the material, k is the wavevector of the mode and t is the thickness of the film.

Both the averaged probe field and the wavevector are functions of the mode shape and mode radius R , so the frequency is obtained by numerical minimization with variation of radius [10]. Due to cylindrical symmetry a zeroth order Bessel function $J_0(kr)$ suitably describes the magnetization profile of the mode, with boundary conditions that define discrete wavevectors $k_n = \chi_n/R$ where χ_n are the zeros of the Bessel function $J_0(\chi_n) = 0$. The minimization of frequency at fixed field is equivalent to the maximization of field at fixed frequency. Hence the deeper field well shifts the modes to higher field when the microwave frequency is fixed, as seen in Fig. 1. This

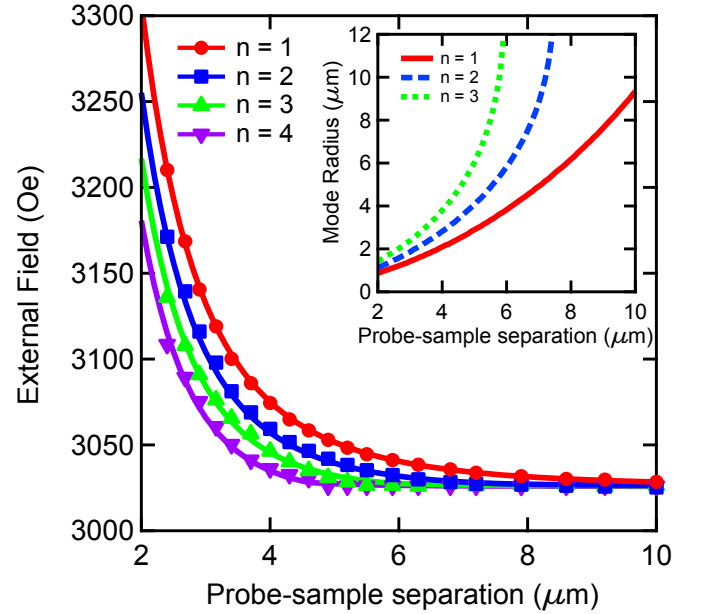


FIG. 2. Resonance field of the first four localized modes as a function of probe-sample separation at 4 GHz. Filled markers indicate experimental peaks and solid lines indicate expected resonance field obtained numerically. Inset: radius of the first three localized modes obtained during the numerical minimization.

modeling procedure provides both the resonance field and the radius of the mode, and these are given in Fig. 2. We see that the resonance fields of the experimental peaks are well described by the model, confirming the accuracy of the calculated mode radius.

To measure damping of a confined mode we obtain FMRFM spectra for a fixed mode radius R at multiple frequencies, one example of which can be seen in Fig. 3. The field shift of the localized modes, relative to the uniform mode $H_{\text{uniform}} = \frac{\omega}{\gamma} + 4\pi M_s$ is constant for a fixed wavevector $k = k_n = \chi_n/R$, independent of frequency ω , as predicted by Equation (1).

By fitting a Lorentzian lineshape to the $n = 1$ peak we obtain the full-width at half-maximum linewidth of the first localized mode and plot this as a function of microwave frequency to separate intrinsic and extrinsic linewidth broadening mechanisms [18]. Following from the Landau-Lifshitz-Gilbert equation, the linewidth ΔH is given by

$$\Delta H = \Delta H_0 + \frac{2\alpha\omega}{\gamma} \quad (2)$$

where the slope of linewidth vs frequency is a measure of the Gilbert damping parameter α and the intercept ΔH_0 is inhomogeneous broadening due to spatial variations in magnetic parameters. We measure this frequency dependence at several probe-sample separations corresponding to several mode radii R .

The key result of our study is the observation of enhanced damping that unambiguously shows a depen-

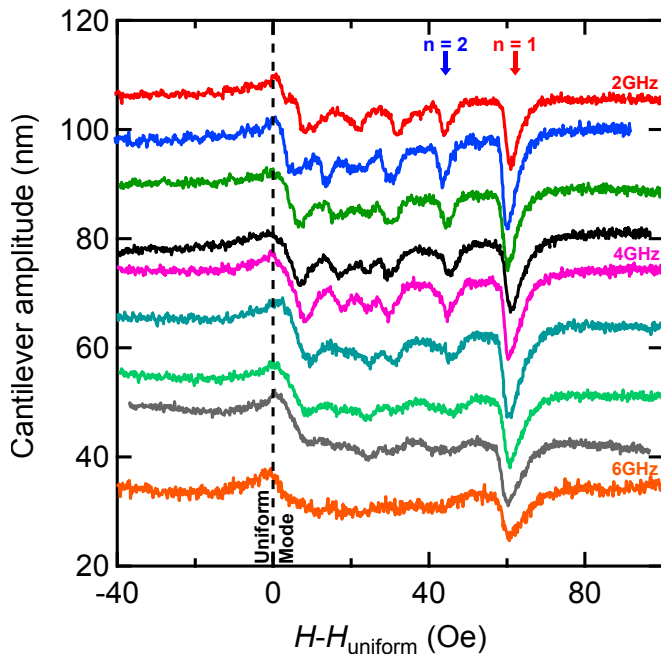


FIG. 3. FMRFM spectra at multiple microwave frequencies at a fixed probe-sample separation of 3700 nm, equivalent to a mode radius $R = 1860$ nm. Spectra are offset for clarity and the external field H is plotted relative to the uniform mode resonance field $H_{\text{uniform}} = \frac{\gamma \hbar \epsilon}{4\pi M_s}$.

dence on the radius of the mode, as seen from the change in slope of linewidth in Fig. 4(a) for several mode radii. The Gilbert damping parameter α shows a surprising linear behavior when plotted against R^{-1} , the reciprocal of the mode radius, as seen in Fig. 4. An enhanced damping is reminiscent of spin pumping observed when a ferromagnetic layer is placed in contact with a normal metal layer [1]. In this bilayer geometry the enhanced damping α_{sp} scales like $1/t$, which equates to the ratio of the area of the interface with the metal to the volume of the ferromagnet, and hence is given by [19]

$$\alpha_{\text{sp}} = \frac{\gamma \hbar g_{\uparrow\downarrow}}{4\pi M_s t} \quad (3)$$

where \hbar is the reduced Planck constant, $g_{\uparrow\downarrow}$ is the spin-mixing conductance parameter that describes the efficiency of spin pumping, and t is the thickness of the ferromagnetic film. As an analogy to this interfacial damping due to spin pumping we suggest the possibility of an interfacial damping mechanism from the volume $\pi R^2 t$ of our disk-like mode which is on resonance to the surrounding material which is off resonance through the curved surface $2\pi R t$ around the edge of the disc. Hence, the enhanced damping should also scale as the surface-to-volume ratio:

$$\alpha_{\text{sp}} = \frac{\gamma \hbar g_{\uparrow\downarrow}}{4\pi M_s R} \quad (4)$$

From Equation (4) and Fig 4, which shows the enhanced damping versus mode radius, we obtain a spin-mixing

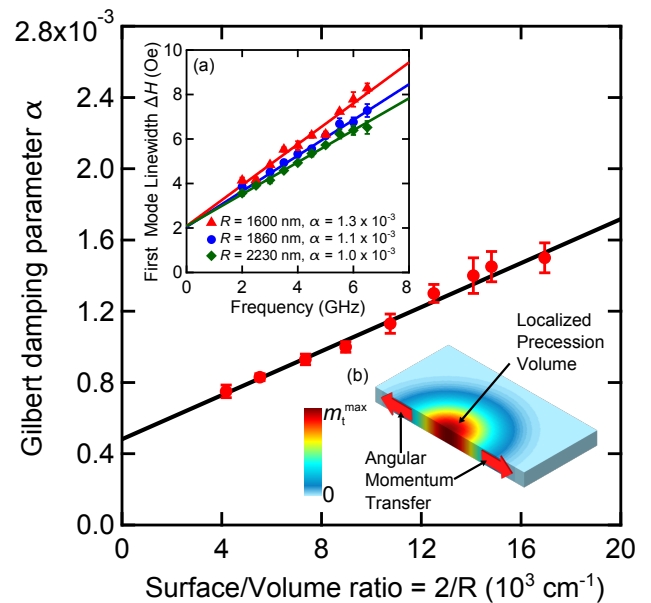


FIG. 4. Gilbert damping parameter α scales inversely with mode radius R equivalent to the surface/volume ratio of the localized mode. (a) Linewidths for mode radii $R = 1600$ nm (red triangles), $R = 1860$ nm (blue squares) and $R = 2230$ nm (green diamonds). Filled markers are experimental linewidths and solid lines are linear fits to the data. Gilbert damping parameters α are determined from the slope of the linear fit. (b) Cross-section showing intralayer angular momentum transfer from the volume of the localized mode to surrounding material through the surface of the mode. Color scale denotes transverse magnetization precession m_t .

conductance for this YIG-YIG system of $g_{\uparrow\downarrow} = (5.3 \pm 0.2) \times 10^{19} \text{m}^{-2}$.

It is interesting and somewhat remarkable that we observe angular momentum transport in this insulating system, and that its efficiency, characterized by an effective spin-mixing conductance $g_{\uparrow\downarrow}$, is larger than that measured in YIG-metal systems [15, 20, 21]. We suggest that $g_{\uparrow\downarrow}$ is a parameter that describes a generalization of spin pumping as the transport of energy and angular momentum from an on-resonance spin source to an off-resonance spin sink, even in the absence of conduction electrons [22]. The energy and angular momentum from the precessing confined mode can be absorbed by the surrounding ferromagnetic material of the unpatterned film, as depicted in Fig. 4(b). The relatively large value for $g_{\uparrow\downarrow}$ we obtain for YIG-YIG compared to values previously measured for YIG-metal [21] can be attributed to the larger exchange coupling in YIG-YIG and that the interface in question is not defined by growth but by a magnetic field. In addition, it might be unexpected for the confined mode to relax via the surrounding material where the lowest energy state, which is the uniform mode, is well above the energy of the confined mode inside the well. However, previous experiments by Heinrich et. al [19, 23] have shown that ferromagnets do act

as good spin sinks when the precession frequency of the spin current is not at a resonance frequency of the spin sink ferromagnet. Lastly, other well-established mechanisms for size- or wavevector-dependent relaxation can be eliminated due to their smaller magnitude and differing phenomenology; 3-magnon confluence [24, 25] manifests as a linewidth broadening that is linear in k but not in frequency, while 4-magnon scattering [26] scales as k^2 .

To conclude, we observe robust intralayer spin pumping within an insulating ferromagnet, which manifests as enhanced damping as the mode radius approaches micron size. This result has consequences for devices that induce spin precession in confined regions, such as spin-torque oscillators in the point-contact geometry [27, 28]. In addition, our study highlights the power of localized mode FMRFM for illuminating local spin dynamics and in particular for spectroscopic studies of the impact of mode relaxation across a controllable, field-defined interface.

The authors wish to thank Yaroslav Tserkovnyak for useful discussions. This work is supported by the Department of Energy (grant No. DE-FG02-03ER46054) (R.A., C.H.D., S.A.M., C.Z. and P.C.H.), the Center for Emergent Materials, an NSF-funded MRSEC (grant No. DMR-0820414) (H.L.W., and F.Y.Y.) and the Army Research Office (grant no. W911NF-09-1-0147) (V.P.B). Partial support is provided by Lake Shore Cryogenics Inc. (C.H.D.). This work was supported in part by an allocation of computing time from the Ohio Supercomputer Center. We also acknowledge technical support and assistance provided by the NanoSystems Laboratory at the Ohio State University.

* fyyang@physics.osu.edu

† hammel@physics.osu.edu

- [1] Y. Tserkovnyak, A. Brataas, and G. E. W. Bauer, *Phys. Rev. Lett.* 88, 117601 (2002).
- [2] A. Brataas, Y. Tserkovnyak, G. E. W. Bauer, and B. I. Halperin, *Phys. Rev. B* 66, 060404 (2002).
- [3] X. Wang, G. E. W. Bauer, B. J. van Wees, A. Brataas, and Y. Tserkovnyak, *Physical Review Letters* 97, 216602 (2006).
- [4] M. Tsoi, A. Jansen, J. Bass, W.-C. Chiang, V. Tsoi, and P. Wyder, *Nature* 406, 46 (2000).
- [5] S. I. Kiselev, J. Sankey, I. Krivorotov, N. Emley, R. Schoelkopf, R. Buhrman, and D. Ralph, *Nature* 425, 380 (2003).
- [6] H. T. Nembach, J. M. Shaw, C. T. Boone, and T. J. Silva, *Phys. Rev. Lett.* 110, 117201 (2013).
- [7] Y. Li and W. E. Bailey, arXiv:1401.6467 [cond-mat.mtrl-sci].
- [8] J. M. Shaw, T. J. Silva, M. L. Schneider, and R. D. McMichael, *Phys. Rev. B* 79, 184404 (2009).
- [9] S. Noh, D. Monma, K. Miyake, M. Doi, T. Kaneko, H. Imamura, and M. Sahashi, *Magnetics, IEEE Transactions on* 47, 2387 (2011).
- [10] I. Lee, Y. Obukhov, G. Xiang, A. Hauser, F. Yang, P. Banerjee, D. V. Pelekhov, and P. C. Hammel, *Nature* 466, 845 (2010).
- [11] H.-J. Chia, F. Guo, L. M. Belova, and R. D. McMichael, *Phys. Rev. Lett.* 108, 087206 (2012).
- [12] E. Nazaretski, D. V. Pelekhov, I. Martin, M. Zalalutdinov, D. Ponarin, A. Smirnov, P. C. Hammel, and R. Movshovich, *Physical Review B (Condensed Matter and Materials Physics)* 79, 132401 (2009).
- [13] G. N. Kakazei, P. E. Wigen, K. Y. Guslienko, V. Novosad, A. N. Slavin, V. O. Golub, N. A. Lesnik, and Y. Otani, *Appl. Phys. Lett.* 85, 443 (2004).
- [14] K. Eason, M. Patricia Rouelli Garcia Sabino, M. Tran, and Y. Fook Liew, *Applied Physics Letters* 102, 232405 (2013).
- [15] H. L. Wang, C. H. Du, Y. Pu, R. Adur, P. C. Hammel, and F. Y. Yang, *Phys. Rev. B* 88, 100406 (2013).
- [16] B. Kalinikos, N. Kovshikov, P. Kolodin, and I. Panchurin, *Elektronnaja Tehnika Ser. 1* 382, 53 (1985).
- [17] E. Schlömann, *Journal of Applied Physics* 35, 159 (1964).
- [18] O. Klein, V. Charbois, V. V. Naletov, and C. Fermon, *Physical Review B (Condensed Matter and Materials Physics)* 67, 220407 (2003).
- [19] B. Heinrich, C. Burrowes, E. Montoya, B. Kardasz, E. Girt, Y.-Y. Song, Y. Sun, and M. Wu, *Phys. Rev. Lett.* 107, 066604 (2011).
- [20] H. Jiao and G. E. W. Bauer, *Phys. Rev. Lett.* 110, 217602 (2013).
- [21] H. Wang, C. Du, Y. Pu, R. Adur, P. Hammel, and F. Yang, arXiv preprint arXiv:1307.2648 (2013).
- [22] C. Hahn, G. De Loubens, V. Naletov, J. B. Youssef, O. Klein, and M. Viret, arXiv:1310.6000 [cond-mat.mtrl-sci].
- [23] B. Heinrich, Y. Tserkovnyak, G. Woltersdorf, A. Brataas, R. Urban, and G. E. W. Bauer, *Phys. Rev. Lett.* 90, 187601 (2003).
- [24] T. Kasuya and R. C. LeCraw, *Phys. Rev. Lett.* 6, 223 (1961).
- [25] M. Sparks, *Ferromagnetic-Relaxation Theory*, Vol. 71 (McGraw-Hill New York, 1964).
- [26] F. J. Dyson, *Phys. Rev.* 102, 1217 (1956).
- [27] M. Madami, S. Bonetti, G. Consolo, S. Tacchi, G. Carlotti, G. Gubbiotti, F. Mancoff, M. A. Yar, and J. Åkerman, *Nature Nanotechnology* 6, 635 (2011).
- [28] V. E. Demidov, S. Urazhdin, H. Ulrichs, V. Tiberkevich, A. Slavin, D. Baither, G. Schmitz, and S. O. Demokritov, *Nature Materials* 11, 1028 (2012).